The Pressurized Cylindrical Crack

T. N. FARRIS*, K. KOKINI** and I. DEMIR*
*School of Aeronautics and Astronautics, **School of Mechanical Engineering, Purdue University, West Lafayette, IN 47907, USA

ABSTRACT

A cylindrical crack in an infinite elastic body is analyzed. The solution procedure reduces the equations of elasticity to two coupled singular integral equations for the Mode I and Mode II dislocation densities which are integrated using numerical quadrature. The stress intensity factors are calculated directly from the dislocation densities. A parameter study reveals that the energy release rate is approximately proportional to the crack radius for crack lengths greater than four times the radius. This result agrees with a simplified model developed using Lame's solution for a pressurized cylinder.

KEYWORDS

Axisymmetry; Crack; Cylindrical; Dislocation; Lame.

INTRODUCTION

The initiation and growth of a cylindrically shaped crack (see Fig. 1) is an important mode of failure for structures made of dissimilar materials with an interface of cylindrical shape. Examples of these are ceramic coatings for high temperature applications(Andersson 1983), glass-to-metal seals in microelectronic components (Kokini and Perkins 1984a), and the fiber/matrix interaction in composite materials (Budiansky *et. al.* 1986). In the first two cases, the structure is subjected to a thermal load that results in tensile radial stresses causing separation and cylindrically shaped cracking, (Kokini and Perkins 1984b). Fiber debonding in unidirectional composites is sometimes induced by interfacial stress concentrations caused by previous damage such as matrix cracking (Budiansky *et. al.* 1986) or broken fibers (Goree and Gross 1980). Additionally, (Atkinson, *et al* 1982) used the cylindrical crack as a model for the fiber pull out test.

The objective of this paper is the accurate analysis of the effect of the cylindrical crack shape on the crack tip stress intensity factors. To this end an infinite elastic body containing a cylindrical crack subjected to internal pressure is analyzed. The solution procedure reduces the elasticity boundary value problem to a system of integral equations whose solution is the dislocation densities. The integral equations are integrated using numerical quadrature and the Mode I and Mode II stress intensity factors are calculated directly from the dislocation densities. After this portion of the research was completed and the paper was submitted, the authors discovered that Erdogan and Ozbek (1969) and Ozbek and

Erdogan (1969) used dislocations to analyze the cylindrical interface crack. Also, Kasano *et al* (1984, 1986) used integral equations to analyze a cylindrical crack in a transversely isotropic body as well as a cylindrical interface crack in an anisotropic body. In this paper strain energy release rates are calculated, using dislocations, and compared to results developed by a simple model based on Lame's solution for a pressurized cylinder.

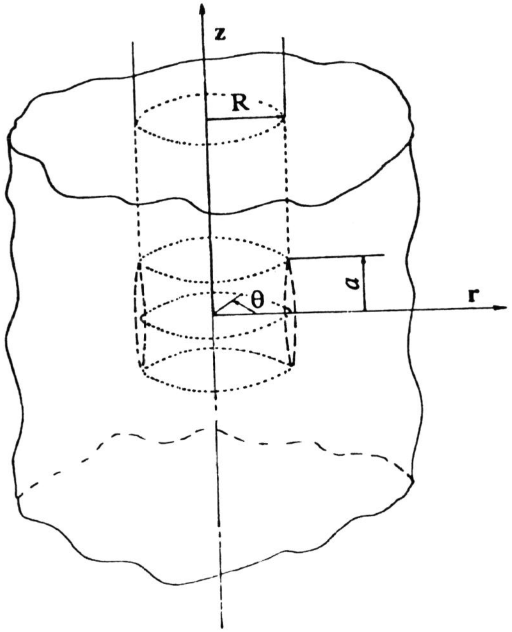

Figure 1. Cylindrical crack and coordinate system

PROBLEM FORMULATION

Love's Stress Function

The problem to be considered is one of torsionless axisymmetry. It is convenient to use Love's stress function ϕ. The stresses and displacements are written in terms of ϕ as

$$\sigma_r = \frac{\partial}{\partial z}(\nu\nabla^2\phi - \frac{\partial^2\phi}{\partial r^2}), \qquad \sigma_\theta = \frac{\partial}{\partial z}(\nu\nabla^2\phi - \frac{1}{r}\frac{\partial\phi}{\partial r}) \tag{1,2}$$

$$\sigma_z = \frac{\partial}{\partial z}[(2-\nu)\nabla^2\phi - \frac{\partial^2\phi}{\partial z^2}], \qquad \sigma_{rz} = \frac{\partial}{\partial r}[(1-\nu)\nabla^2\phi - \frac{\partial^2\phi}{\partial z^2}] \tag{3,4}$$

$$2Gu = -\frac{\partial^2\phi}{\partial r\partial z}, \qquad 2Gw = 2(1-\nu)\nabla^2\phi - \frac{\partial^2\phi}{\partial z^2} \tag{5,6}$$

where

$$\nabla^2\nabla^2\phi = 0 \tag{7}$$

ensures that equilibrium is satisfied, σ represents the components of stress in cylindrical coordinates (Fig. 1), u is the radial (r) displacement, w is the axial (z) displacement, G is the shear modulus, and ν is Poisson's ratio. The angular (θ) displacement, $\sigma_{r\theta}$, and $\sigma_{\theta z}$ are identically zero.

Equation (7) is integrated through the use of the Fourier Transform pair

$$\hat{\phi}(r;\xi) = \frac{1}{\sqrt{2\pi}}\int_{-\infty}^{\infty}\phi(r,z)e^{i\xi z}dz, \qquad \phi(r,z) = \frac{1}{\sqrt{2\pi}}\int_{-\infty}^{\infty}\hat{\phi}(r;\xi)e^{-i\xi z}dz \tag{8,9}$$

where $i = \sqrt{-1}$. Applying the Fourier Transform to Eqn. (7) and integrating the resulting differential equation yields

$$\xi^2\hat{\phi}(r;\xi) = A(\xi)I_0(\xi r) + B(\xi)\xi r I_1(\xi r) + C(\xi)K_0(\xi r) + D(\xi)\xi r K_1(\xi r) \tag{10}$$

where I and K are Modified Bessel functions of the first and second kind respectively, (Abramowitz and Stegun 1968). It is noted that for our purposes we define $I_0(-\xi r) \equiv I_0(\xi r)$, $I_1(-\xi r) \equiv -I_1(\xi r)$, $K_0(-\xi r) \equiv K_0(\xi r)$, and $K_1(-\xi r) \equiv -K_1(\xi r)$. The transform parameters $A(\xi)$, $B(\xi)$, $C(\xi)$, and $D(\xi)$ are chosen to satisfy the boundary conditions.

Before the inverse transform representations for the stresses and displacements are written it is convenient to separate the cracked body (Fig. 1) into region 1 for $r<R$ and region 2 for $r>R$. To ensure that the stresses and displacements are bounded as $r\to 0$ and $r\to\infty$, $C(\xi)$ and $D(\xi)$ are set to zero in region 1 and $A(\xi)$ and $B(\xi)$ are set to zero in region 2. Substitution of Eqn. 10 into Eqn. 9 allows the stresses and displacements to be written as

$$2Gu^1 = \frac{i}{\sqrt{2\pi}}\int_{-\infty}^{\infty}[AI_1(\xi r) + B\xi r I_0(\xi r)]e^{-i\xi z}d\xi \tag{11}$$

$$2Gw^1 = \frac{1}{\sqrt{2\pi}}\int_{-\infty}^{\infty}\{AI_0(\xi r) + B[4(1-\nu)I_0(\xi r) + \xi r I_1(\xi r)]\}e^{-i\xi z}d\xi \tag{12}$$

$$\sigma_r^1 = \frac{-i}{\sqrt{2\pi}}\int_{-\infty}^{\infty}\xi\{A[\frac{I_1(\xi r)}{\xi r} - I_0(\xi r)] - B[(1-2\nu)I_0(\xi r) + \xi r I_1(\xi r)]\}e^{-i\xi z}d\xi \tag{13}$$

$$\sigma_\theta^1 = \frac{i}{\sqrt{2\pi}}\int_{-\infty}^{\infty}\xi[A\frac{I_1(\xi r)}{\xi r} + B(1-2\nu)I_0(\xi r)]e^{-i\xi z}d\xi \tag{14}$$

$$\sigma_z^1 = \frac{-i}{\sqrt{2\pi}}\int_{-\infty}^{\infty}\xi\{AI_0(\xi r) + B[2(2-\nu)I_0(\xi r) + \xi r I_1(\xi r)]\}e^{-i\xi z}d\xi \tag{15}$$

$$\sigma_{rz}^1 = \frac{1}{\sqrt{2\pi}}\int_{-\infty}^{\infty}\xi\{AI_1(\xi r) + B[2(1-\nu)I_1(\xi r) + \xi r I_0(\xi r)]\}e^{-i\xi z}d\xi \tag{16}$$

$$2Gu^2 = \frac{-i}{\sqrt{2\pi}}\int_{-\infty}^{\infty}[CK_1(\xi r) + D\xi r K_0(\xi r)]e^{-i\xi z}d\xi \tag{17}$$

$$2Gw^2 = \frac{1}{\sqrt{2\pi}}\int_{-\infty}^{\infty}\{CK_0(\xi r) - D[4(1-\nu)K_0(\xi r) - \xi r K_1(\xi r)]\}e^{-i\xi z}d\xi \tag{18}$$

$$\sigma_r^2 = \frac{i}{\sqrt{2\pi}}\int_{-\infty}^{\infty}\xi\{C[\frac{K_1(\xi r)}{\xi r} + K_0(\xi r)] + D[\xi r K_1(\xi r) - (1-2\nu)K_0(\xi r)]\}e^{-i\xi z}d\xi \tag{19}$$

$$\sigma_\theta^2 = \frac{-i}{\sqrt{2\pi}}\int_{-\infty}^{\infty}\xi[C\frac{K_1(\xi r)}{\xi r} + D(1-2\nu)K_0(\xi r)]e^{-i\xi z}d\xi \tag{20}$$

$$\sigma_z^2 = \frac{-i}{\sqrt{2\pi}}\int_{-\infty}^{\infty}\xi\{CK_0(\xi r) + D[-2(2-\nu)K_0(\xi r) + \xi r K_1(\xi r)]\}e^{-i\xi z}d\xi \tag{21}$$

$$\sigma_{rz}^2 = \frac{1}{\sqrt{2\pi}}\int_{-\infty}^{\infty}\xi\{-CK_1(\xi r) + D[2(1-\nu)K_1(\xi r) - \xi r K_0(\xi r)]\}e^{-i\xi z}d\xi \tag{22}$$

where A, B, C, and D are as yet unknown functions of ξ and the superscripts refer to the different regions of the body.

Boundary Conditions

An infinite elastic body contains a cylindrically shaped crack of radius R and length $2a$. The crack is loaded by internal pressure of magnitude p. The appropriate boundary conditions are given next along with conditions for continuity between regions 1 and 2:

$$\sigma_r^1(R,z)=\sigma_r^2(R,z)\,,\qquad \sigma_{rz}^1(R,z)=\sigma_{rz}^2(R,z)\,,\qquad -\infty<z<\infty \tag{23,24}$$

$$\sigma_r^1(R,z)=-p\,,\qquad \sigma_{rz}^1(R,z)=0\,,\qquad -a<z<a \tag{25,26}$$

$$u^1(R,z)=u^2(R,z)\,,\qquad w^1(R,z)=w^2(R,z)\,,\qquad |z|>a \tag{27,28}$$

The continuity of stresses, Eqns. (23-24), allow A and B to be written in terms of C and D. The continuity of displacements, Eqns. (27-28), is satisfied by writing the jump in the displacement across the crack in terms of dislocation densities as

$$-\frac{\partial}{\partial z}\,[u^2(R,z)-u^1(R,z)]=B_1(z)\,H(a-|z|) \tag{29}$$

$$-\frac{\partial}{\partial z}\,[w^2(R,z)-w^1(R,z)]=B_2(z)\,H(a-|z|) \tag{30}$$

where H is the Heaviside step function equal to unity for positive argument and zero for negative argument. Next C and D are written in terms of the Fourier Transforms of B_1 and B_2. The resulting forms of C and D are substituted into the crack face traction conditions, Eqns. (25-26), yielding, after some manipulation:

$$-\int_{-a}^{a}\frac{B_1(s)ds}{s-z}+\int_{-a}^{a}B_1(s)L_1(s,z)ds-\int_{-a}^{a}B_2(s)L_2(s,z)ds=-\frac{2\pi(1-\nu)p}{G}\,,\quad -a<z<a \tag{31}$$

$$-\int_{-a}^{a}\frac{B_2(s)ds}{s-z}+\int_{-a}^{a}B_1(s)L_2(s,z)ds-\int_{-a}^{a}B_2(s)L_3(s,z)ds=0\,,\quad -a<z<a \tag{32}$$

where the kernels L_1, L_2, and L_3 are given in the APPENDIX. The continuity of displacements outside the crack requires that the net dislocation is zero giving

$$\int_{-a}^{a}B_1(s)ds=0,\qquad \int_{-a}^{a}B_2(s)ds=0 \tag{33,34}$$

Numerical Quadrature

The problem is reduced to inverting the system of integral equations , Eqns. (31-34), for the unknown dislocation densities. The kernels are continuous for $-a<s<a$ and $-a<z<a$ so that the square root singularity at $z=|a|$ in the dislocation densities is determined by the first term in Eqns. (31-32). This singularity is the same as that for the dislocation densities relevant to a straight plane strain crack. Following Gerasoulis (1982), Eqns. (31-34) are nondimensionalized by

$$s=a\bar{s}\,,\ z=a\bar{z} \tag{35}$$

$$B_1(a\bar{s})=\frac{2\pi(1-\nu)}{G}p\frac{\bar{B}_1(\bar{s})}{\sqrt{1-\bar{s}^2}},\qquad B_2(a\bar{s})=\frac{2\pi(1-\nu)}{G}p\frac{\bar{B}_2(\bar{s})}{\sqrt{1-\bar{s}^2}} \tag{36,37}$$

The equations are integrated by approximating $\bar{B}_1$ and $\bar{B}_2$ as piecewise quadratic. Once $\bar{B}_1$ and $\bar{B}_2$ are calculated, the Mode I and Mode II stress intensity factors are calculated through

$$K_I(a)\equiv\lim_{z\to a^+}\sqrt{2\pi(z-a)}\,\sigma_r(R,z)=p\sqrt{\pi a}\,\pi\bar{B}_1(1) \tag{38}$$

$$K_{II}(a)\equiv\lim_{z\to a^+}\sqrt{2\pi(z-a)}\,\sigma_{rz}(R,z)=p\sqrt{\pi a}\,\pi\bar{B}_2(1) \tag{39}$$

NUMERICAL RESULTS

The stress intensity factors normalized by $\bar{K}_I$ for a plane strain crack of length $2a$ subjected to internal pressure p, $\bar{K}_I=p\sqrt{\pi a}$, are shown in Fig. 2 as a function of R/a and ν. The value for K_I is the same for each crack tip and $K_{II}(a)=-K_{II}(-a)$. For large R/a, K_I approaches $\bar{K}_I$ and K_{II} goes to zero. As the radius decreases K_I reduces relative to its value for a plane strain crack of the same length and K_{II} first increases then decreases in absolute value. Note that for ν=.25 and ν=.5 the sign of $K_{II}(a)$ is negative. This sign suggests that if the crack were to grow it would tend to grow away from its center. That is, any crack growth would not be self similar and the crack would grow at an angle into region 2.

Fig. 2 also shows K_I and K_{II} normalized by $\sqrt{\pi R}$. For large values of a/R, $K_I/p\sqrt{\pi R}$ and $K_{II}/p\sqrt{\pi R}$ become approximately horizontal lines. This fact is discussed further in the DISCUSSION section.

DISCUSSION

Next, an approximate calculation of the energy release rate for plane strain,

$$G\equiv\frac{1-\nu^2}{E}\,(K_I^2+K_{II}^2) \tag{40}$$

is outlined. The approximate solution is based on Lame's solution for a pressurized cylinder. The approximate calculation ignores the strain energy caused by deformation in the regions $|z|>a$ and is a more appropriate approximation for large values of a/R.

Region 1, $r<R$ is treated as a solid cylinder of length $2a$ and radius R subjected to external pressure

$$\sigma_r(R,z)=-p,\qquad \sigma_{rz}(R,z)=0 \tag{41,42}$$

The ends of the cylinder are constrained leading to plane strain conditions. The strain energy

$$U=\frac{1}{2}\int_V\sigma_{ij}\varepsilon_{ij}\,dV \tag{43}$$

is calculated as

$$U^1=2\pi aR^2\frac{p^2}{E}\,[\,(1-\nu)-2\nu^2\,] \tag{44}$$

Region 2 is treated as an infinite elastic body containing a circular hole of radius R, subjected to internal pressure p. Again plane strain assumptions lead to

$$U^2=2\pi aR^2\,\frac{p^2}{E}\,(1+\nu) \tag{45}$$

The total strain energy in the body is

$$U=U^1+U^2=4\pi aR^2\,\frac{p^2}{E}\,(1-\nu^2) \tag{46}$$

The strain energy release rate is defined as $G=\dfrac{\partial U}{\partial A}$ where A is the area of the crack faces.

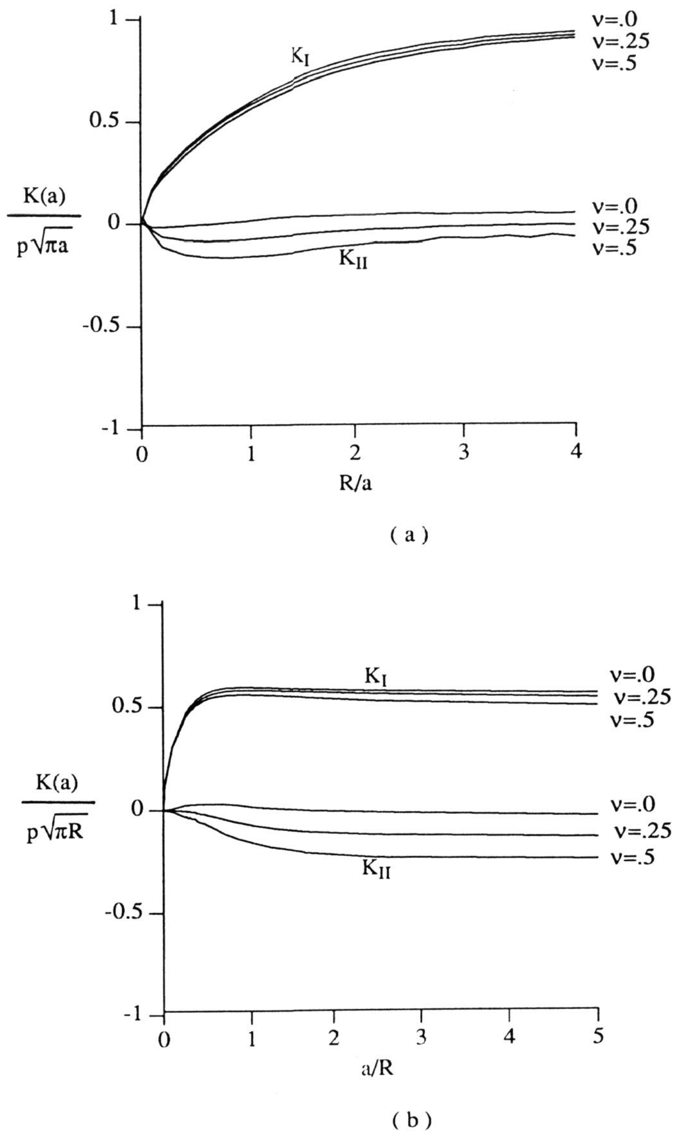

Fig. 2. Mode I and Mode II stress intensity factors.

The assumption of self similar growth (R constant) leads to

$$G = \frac{(1-\nu^2)}{E}\, p^2 R \tag{47}$$

The energy release for plane strain crack of length $2a$ in an infinite body subjected to internal pressure p is

$$G = \frac{(1-\nu^2)}{E}\, p^2 \pi a \tag{48}$$

Equations (40,47,48) for G are shown in Fig. 3. The Lame approximation works well for $a/R > 2$. It is striking to note that G is independent of a for $a/R > 2$. For comparison, results from Kasano *et al* (1984) using Eqn. (40) are also given in Fig. 3.

CONCLUSION

The fundamental problem of a cylindrical crack subjected to internal pressure is analyzed. It is found that the cylindrical geometry reduces the Mode I stress intensity factor relative to that for a plane strain crack of the same length. In addition, the cylindrical geometry induces a Mode II stress intensity factor causing mixed-mode deformation of the crack faces. For crack lengths larger than four times the crack radius, the energy release rate becomes proportional to the crack radius. An approximate model based on Lame's pressurized cylinder solution verified this result.

The solution presented here for internal crack pressure can be used with the superposition principle to calculate stress intensity factors for additional loadings. Alternative crack face loadings such as nonuniform pressure and shear tractions, σ_{rz}, can easily be incorporated in the analysis.

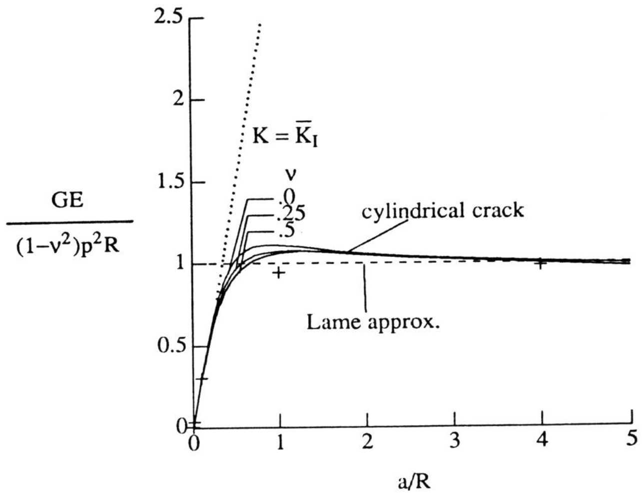

Fig. 3. Comparison of energy release rates, the + are from Kasano *et al* (1984) for $\nu = 0.3$.

REFERENCES

Abramowitz, M. and Stegun, I.A., (1972). *Handbook of Mathematical Functions,* 9th Printing, Dover, New York, Chaps. 9 and 25.

Andersson, C.A., (1983). Thermal stress fracture of ceramic coatings. *Fracture Mechanics of Ceramics,* 6, Eds: Bradt, Evans, Hasselman, and Lange, Plenum Press, N.Y. pp 497-509.

Atkinson, C., Avila, J., Betz, E., and Smelser, R.E., (1982). The rod pull out problem, theory and experiment. *J. Mech. Phys. Solids.* 30, 97-120.

Budiansky, B., Hutchinson, J.W. and Evans, A.G., (1986). Matrix fracture in fiber-reinforced ceramics. *J. Mech. Phys. Solids,* 34, 167-189.

Erdogan, F. and Ozbek, T. (1969). Stresses in fiber-reinforced composites with imperfect bonding. *J. Appl. Mech.,* 36, 865-869.

Gerasoulis, A., (1982). The use of piecewise quadratic polynomials for the solution of singular integral equations of Cauchy type. *Comput. Math. Appl.,* 8, 15-19.

Goree, J.G. and Gross, R.S., (1980). Stresses in a three-dimensional unidirectional composite containing broken fibers. *Engng. Fracture Mech.,* 13, 395-405.

Kasano, H., Matsumoto, H., and Nakahara, I., (1984). A torsion-free axisymmetric problem of a cylindrical crack in a transversely isotropic body. *Bulletin of JSME,* 27, 1323-1332.

Kasano, H., Matsumoto, H., and Nakahara, I., (1986). A cylindrical interface crack in a nonhomogeneous anisotropic elastic body. *Bulletin of JSME,* 29, 1973-1981.

Kokini, K. and Perkins, R.W., (1984a). Estimating the strength of annular glass-to-metal seals in microelectronic packages: an experimental study. *IEEE Trans on Components, Hybrids, and Manufacturing Technology,* CHMT–7, 276-280.

Kokini, K and Perkins, R.W., (1984b). Thermal stresses in annular glass-to-metal seals under thermal shock. *AIAA Journal,* 22, 1472-1477.

Ozbek, T., Erdogan, F., (1969). Some elasticity problems in fiber-reinforced composites with imperfect bonds. *Int. J. Engng. Sci.,* 7, 931-946.

APPENDIX

The continuous portion of the integral equation kernels are given by

$$L_1(s,z) = 2\int_0^\infty \{[2\xi R\,(K_1I_1 - K_0I_0) + (3-2\nu)(K_0I_1 - K_1I_0) + \xi^2R^2(K_0I_1 - K_1I_0) + \frac{4(1-\nu)}{\xi R}K_1I_1] + \frac{1}{2}\}\sin[\xi(s-z)]d\xi \quad \text{(A1)}$$

$$L_2(s,z) = 2\int_0^\infty [\xi R\,(K_0I_1 - K_1I_0) + \xi^2R^2(K_1I_1 - K_0I_0) + 2(1-\nu)K_1I_1] \times \cos[\xi(s-z)]d\xi \quad \text{(A2)}$$

$$L_3(s,z) = 2\int_0^\infty \{\xi^2R^2(K_1I_0 - K_0I_1) - \frac{1}{2}\}\sin[\xi(s-z)]d\xi \quad \text{(A3)}$$

where $I_0 = I_0(\xi R)$, $I_1 = I_1(\xi R)$, $K_0 = K_0(\xi R)$, and $K_1 = K_1(\xi R)$. These integrals are evaluated numerically using Filon's Method (Abramowitz and Stegun 1972).